p = total vapor pressure
p_i^s = vapor pressure of pure component i
R = gas constant
S^E = molar excess entropy
T = absolute temperature
U_V^E = molar excess energy at constant volume
V^E = molar excess volume
V_i^s = molar volume of pure component i
X^E = typical molar excess property
x_i = mole fraction of component i in liquid phase
y_i = mole fraction of component i in vapor phase

Greek Letters

α = coefficient of thermal expansion
β = coefficient of isothermal compressibility
γ_i = activity coefficient of component i in liquid phase
δ = difference of virial coefficients, as defined in Equation 3
δ_i = solubility parameter of component i
ϕ_i = volume fraction of component i, referred to unmixed state
σ, σ_x, σ_y, σ_p, σ_U = standard errors

LITERATURE CITED

(1) American Petroleum Institute, Research Project 44, "Selected Values of Properties of Hydrocarbons and Related Compounds," Carnegie Press, Carnegie Institute of Technology, Pittsburgh, Pa., 1953, and later revisions.
(2) Boublik, T., Benson, G.C., *Can. J. Chem.* **47**, 539 (1969).
(3) Boublik, T., Lam, V.T., Murakami, S., Benson, G.C., *J. Phys. Chem.* **73**, 2356 (1969).
(4) Bridgeman, O.C., Aldrich, E.W., *J. Heat Transfer* **86**, 279 (1964).
(5) Dreisbach, R.R., *Advan. Chem. Ser.* No. **22** (1959).
(6) Dreisbach, R.R., Martin, R.A., *Ind. Eng. Chem.* **41**, 2875 (1949).
(7) Erdös, E., *Collection Czechoslov. Chem. Commun.* **21**, 1528 (1956).
(8) Fried, V., Franceschetti, D.R., Gallanter, A.S., *J. Phys. Chem.* **73**, 1476 (1969).
(9) Fried, V., Franceschetti, D.R., Schneier, G.B., J. CHEM. ENG. DATA **13**, 415 (1968).
(10) Fried, V., Gallant, P., Schneier, G.B., *Ibid.*, **12**, 504 (1967).
(11) Hermsen, R.W., Prausnitz, J.M., *Chem. Eng. Sci.* **18**, 485 (1963).
(12) Hildebrand, J.H., Scott, R.L., "Regular Solutions," Chap. 7, Prentice-Hall, Englewood Cliffs, N. J., 1962.
(13) "International Critical Tables," Vol. **III**, McGraw-Hill, New York, 1928.
(14) Kohler, F., *Monatsh. Chem.* **88**, 857 (1957).
(15) McGovern, E.W., *Ind. Eng. Chem.* **35**, 1230 (1943).
(16) Murakami, S., Benson, G.C., *J. Chem. Thermodynamics* **1**, 559 (1969).
(17) O'Connell, J.P., Prausnitz, J.M., *Ind. Eng. Chem. Process Design Develop.* **6**, 245 (1967).
(18) Pflug, H.D., Benson, G.C., *Can. J. Chem.* **46**, 287 (1968).
(19) Pitzer, K.S., Curl, R.F., *J. Am. Chem. Soc.* **79**, 2369 (1957).
(20) Polák, J., *Collection Czechoslov. Chem. Commun.* **31**, 1483 (1966).
(21) Poon, D.P.L., Lu, B.C-Y., J. CHEM. ENG. DATA **13**, 435 (1968).
(22) Redlich, O., Kister, A.T., *Ind. Eng. Chem.* **40**, 345 (1948).
(23) Reid, R.C., Sherwood, T.K., "Properties of Gases and Liquids," 2nd ed., McGraw-Hill, New York, 1966.
(24) Timmermans, J., "Physico-Chemical Constants of Pure Organic Compounds," Vol. **I**, Elsevier, New York, 1950.

RECEIVED for review October 14, 1969. Accepted December 29, 1969. Issued as N.R.C.C. No. 11255.

Measurements of Gaseous Diffusion Coefficients for Dilute and Moderately Dense Gases by Perturbation Chromatography

ALEXANDER TZI-CHIANG HU and RIKI KOBAYASHI
Department of Chemical Engineering, William Marsh Rice University, Houston, Tex. 77001

THE DIFFUSION COEFFICIENT, $\mathscr{D}$, has various definitions dependent upon the theoretical assumptions—i.e., kinetic theory, Fick's laws, molecular transport, etc. However, at infinite dilution, the conditions of this study, all the definitions become equal (*35*). Extensive discussions are available in standard references (*12, 23, 37*).

The dispersion of a very small (infinite dilution) amount of solute injected into a steady-state stream of solvent flowing through a tube is comprised of two effects: the dispersion due to molecular diffusion and the dispersion induced by the velocity profile of the steady-state stream combined with any geometrical effects of the system. For the case of laminar flow of a Newtonian fluid in a circular tube of infinite length, the effective diffusion coefficient is defined (*3, 43*) as

$$\mathscr{D}_e = \mathscr{D} + (\bar{u}\, r_t)^2/(48\mathscr{D}) \qquad (1)$$

Diffusivity, $\mathscr{D}_e$, is a function of the variance. The variance, σ^2, defined in Equation 5, is a function of the distribution of the concentration of the injected solute down the tube from the injection point, as determined by the elapsed time and flow rate of the solvent.

There are two roots for $\mathscr{D}$ in Equation 1, only one of which satisfies the condition that the diffusivity is independent of the flow rate. Previous investigators (*18*) stated that up to the critical flow rate the larger (positive) root should be taken; however, careful examination of Figure 1 will show that this is not a satisfactory criterion, because the critical flow is not calculable without additional information. Subscripts 1 and 2 in Figure 1 refer to measurements at two different flow rates. Both roots for the diffusivity and the associated critical velocities are indicated. Either measurements at two different flow rates or a knowledge of the magnitude of $\mathscr{D}$ is required to determine the correct root.

PREVIOUS WORK

The second term of Equation 1 was first measured by Taylor (*43*) in a liquid system. Some gaseous diffusion

Measurements based on the dispersion model for laminar flow in a long circular tube were conducted up to 60 atm at 24° C for tritiated methane in methane and in tetrafluoromethane; and at 50°, 25°, 0°, and −25° C for argon in helium, carbon dioxide in helium, methane in helium, and nitrogen in helium. Perturbation detection improvements included radioactive detection by a small volume ionization chamber and nonradioactive detection by a microthermal conductivity cell. Agreement between experimental and theoretical values was good for variance calculations. Density-diffusivity products of the systems studied were independent of the density over the pressure range investigated. Two experimental methods yielding the same results were used: the multiflow rate method, which used several velocities at the same temperature and pressure, and the one-flow rate method, which required measurements at only one flow rate.

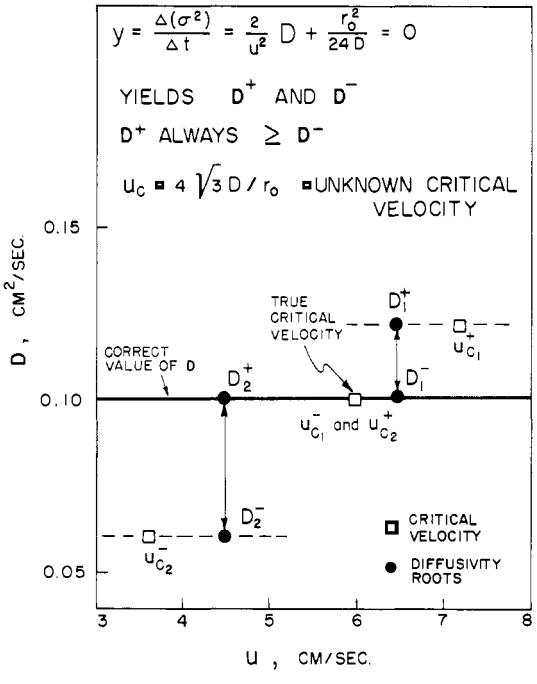

Figure 1. Selection of correct root for diffusivity

measurements by Bournia (*7*) using a similar technique in 1961 were shown in 1965 to be unsatisfactory (*17*) because of erroneous sampling techniques. A method using two tubes of different lengths was used by Giddings and Seager (*18*), with the assumption that gaseous diffusion values could be obtained by the difference in the variance for each tube. Their values, although somewhat widely scattered because of difficulties in flow rate control and measurements, were in reasonable agreement with results of other investigators.

The effect of a coiled column for a tube-to-column inside diameter ratio of 0.01 to 0.033 was found significant by van Andel, Kramers, and de Voogd (*1*) when the Reynolds number exceeds 100. Measurements by Evans and Kenney (*17*) of some gaseous diffusivities with a long straight tube confirmed the solution of Aris (*3*) at low pressure. Studies of dilute and moderately dense gaseous diffusion by Chang and Kobayashi (*10, 11*) showed that additional improvements were needed for diffusion coefficient measurements by perturbation techniques.

DEVELOPMENT OF MATHEMATICAL RELATIONSHIPS

The basic relationship for gaseous diffusion in a long circular tube with a laminar flowing Newtonian fluid is

$$\frac{\partial C}{\partial \tau} = \frac{\partial^2 C}{\partial \rho^2} + \frac{1}{\rho}\frac{\partial C}{\partial \rho} + \frac{\partial^2 C}{\partial x_1^2} + \frac{\mathrm{Pe}}{2}(1 - 2\rho^2)\frac{\partial C}{\partial x_1} \qquad (2)$$

The boundary conditions are two: At the center of the tube ($\rho = 0$) concentration C is finite, and at the edge of the flowing fluid ($\rho = 1$) the mass flux is zero ($\partial C/\partial \rho = 0$).

With the restriction that the flow diffusion is much larger than the molecular diffusion, an analysis by Taylor (*43, 44*) in 1953 of Equation 2 yielded the second term of Equation 1, which is commonly known as Taylor's diffusion. Without this restriction, the more general case for an infinitely long tube of no specific geometry was treated by Aris (*3, 4*) through the moment technique. For a circular tube his result for the second moment is

$$\frac{dm_2}{d\tau} = 2\frac{\mathscr{D}_e}{\mathscr{D}} + O\left[\exp\left(-a\tau\right)\right] \qquad (3)$$

For all experimental systems τ will be large, and the second term of Equation 3 will approach zero and become negligible. Later analysis by Gill and Ananthakrishnan (*19*) yielded both a numerical solution for a finite slug input and a table of approximate values of τ as a function of the Peclet number, for which Equation 3 is valid.

For a tube of finite length, with the assumption that the concentration over the cross section of the tube is nearly constant, Golay (*20*) modified Equation 2 to obtain

$$\mathscr{D}_e\left[\frac{\partial^2 \overline{C}}{\partial(z - \overline{u}t)^2}\right] = \frac{\partial \overline{C}}{\partial t} \qquad (4)$$

For a delta or "instantaneous" injection, Levenspiel and Smith (*29*) showed that from Equation 4 the detected concentration response or variance is given by

$$(\sigma^2) = 2\alpha(1 + 4\alpha)(L/\overline{u})^2 \qquad (5)$$

For α less than 0.01, van der Laan (*28*) showed that end effects of a finite tube can be ignored. To account for the fact that the injection of a delta function is only approximately possible, Bischoff (*5*) proposed that measurement on two tubes of different lengths would yield the mean time, $\overline{t}$, and the variance, σ^2. Bischoff and Levenspiel (*6*) made an order of magnitude estimate for the limitation of the theory. Some independent experimental investigations (*10, 11, 18*) applied the same two-tube idea in performing measurements. Arai, Saito, and Maeda (*2*) presented a theoretical analysis of the effects of the injection valve and the detector.

For a real experimental system, two inevitable effects which exist are:

1. The injection effect is completely contained in a very small injection region at $x_1 = x_0$ and $\tau = 0$.
2. There is a detector effect at $x_1 = x_L$.

In addition, previous theoretical studies have shown that the experimental study of diffusion requires additional considerations.

3. The second term in Equation 3 must be effectively zero—i.e., τ must be large so that $\mathscr{D}_e$ is a constant with respect to tube length.

4. The Golay assumption of nearly constant cross-sectional concentration, Equation 4, has to be justified for each system.

5. A perfect delta injection is not necessary with two-point measurements downstream from the injection point, or with two tubes of different length and the same radii lengths.

6. The use of small injection and detection devices can reduce the first and second effects.

With these six conditions, from Equation 5 we obtain

$$\frac{\Delta(\sigma^2)}{\Delta L} = \frac{2}{\bar{u}^3}\left(\mathscr{D} + \frac{r_t^2\bar{u}^2}{48\mathscr{D}}\right) \tag{6}$$

For α less than 0.001 (*29*) and for a small sample injection (*2*), the concentration distribution becomes close to Gaussian. The characteristics of the concentration profile can be assumed to have linearized Gaussian characteristics y and w of the type

$$w^2 = -8\,(\sigma^2 + a_1)\,\ln y + a_2 \tag{7}$$

$$t_r = L/\bar{u} + a_3 \tag{8}$$

From Equations 6, 7, and 8, this experimental system for several flow rates at the same temperature and pressure, which is defined as the multiflow rate method, is represented by

$$\frac{\Delta(\sigma^2)}{\Delta t_r} = \frac{2}{\bar{u}^2}\mathscr{D} + \frac{\beta}{\mathscr{D}} \tag{9}$$

Or, for one measurement at a set of conditions, which is defined as the one-flow rate method, this experimental system is given by

$$\frac{\Delta(\sigma^2)}{\Delta t_r} = \frac{2}{\bar{u}^2}\mathscr{D} + \frac{r_t^2}{24\mathscr{D}} \tag{10}$$

Equation 10 represents the working relations for the variance with the foregoing assumptions and may be applied to obtain the molecular diffusivity from measurements at only one flow rate.

EXPERIMENTAL APPARATUS

A schematic diagram of the apparatus, described in more detail elsewhere (*25*), is given in Figure 2. The fixed apparatus was placed on a platform within a frame, above the constant temperature bath contained in a stainless steel Dewar flask fixed in a metal box, which could be raised into position under operating conditions. All lines, valves, etc., were constructed of stainless steel.

Temperature System. Bath fluids used were L-45 silicone oil and isohexanes. Two stirrers were used to achieve an improved (*10, 11*) circulation pattern of the bath fluid. Temperature measurement at two points within the bath was taken. At 50° C precision Tagliabue Co. total immersion thermometers with certifications of 50° C = 50.00 and 122° F = 121.98 were used with scale markings of 0.2°, and at the lower temperatures readings were taken by a 10-junction Chromel-Constantan thermopile calibrated (*10, 11*) against a platinum resistance thermometer to give measurements to 0.01° F. Constant temperature within ±0.01° variation for a 1-hour period was achieved by the combination of constant cooling with variable heating controlled by the Thermotrol, sensitive to ±0.004°.

Pressure System. The system was observed over several days to maintain the maximum pressure before data were

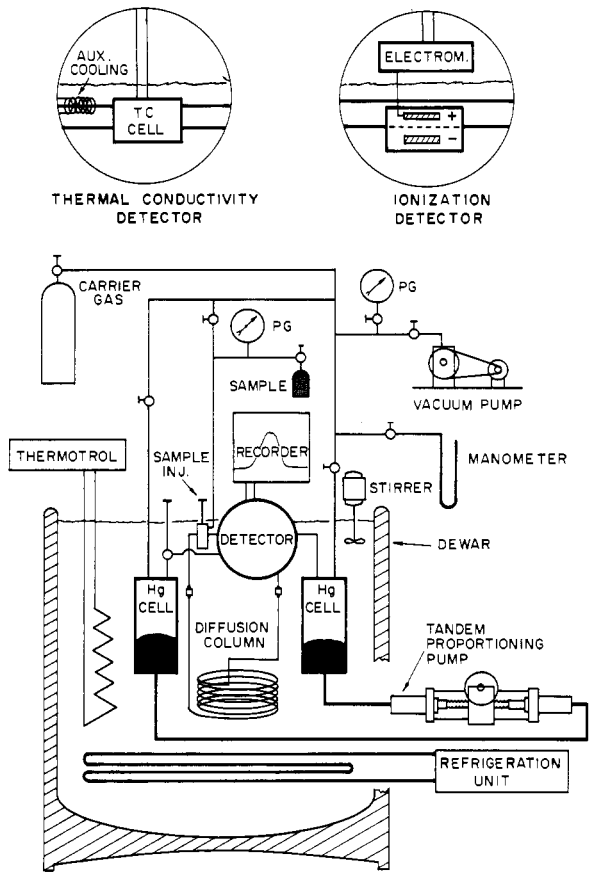

Figure 2. Schematic diagram of diffusion apparatus

taken. Pressures below 3 atm were measured with a mercury manometer. Heise Bourdon tube gages of 200-, 500-, and 2000-psi ranges (*PG*, Figure 2) were used at the higher pressures. The calibration of the Heise gages was verified to be within the Heise tolerance of 0.1% with a dead-weight gage.

Sample System. The high pressure sample injection valve, which introduced the pulse of tracer into the carrier gas, was completely immersed in the bath fluid, so that the sample was at the system temperature. The sample valve of 10-μl volume was designed for pressures up to 67 atm by Micro-Tek Instrument, Inc. Teflon sealing rings were substituted for the O-rings, in order that the valve could be placed into the bath fluid.

Diffusion Columns. A 14-cm-diameter coiled column made of precision-drawn ⅛-inch o.d. Type 304 S.S. tubing purchased from J. Bishop Co., Malvern, Pa., was cut into various lengths to serve as the diffusion columns. The tubing was taken from the same lot as that used by Chang (*10, 11*), who determined the free cross-sectional area to be 0.04459 ± 0.00007 cm^2 and the radius to be 0.1191 ± 0.0001 cm by the retention time method. This study used longer tubes than Chang in order to approach a Gaussian distribution (*29*) more closely.

Thermal Conductivity Detector (T.C. Cell). For the nontracer gases, the difference in the heat transfer between the elution and perturbation gases was used to detect the perturbation of the sample. The cell was a Model 470 microthermistor cell manufactured by Gow-Mac Instrument Co., Madison, N. J. The cell had a 0.025-cc sensing volume and a response time of less than 0.5 second. The entire cell was located within the bath, with the bath fluid circulation carefully directed around the cell to achieve the desired constant temperature. As shown in Figure 2, after the carrier gas line flowed through the reference side of the T.C. cell, an additional auxiliary cooling column within the bath

cooled the gas to the system temperature before the sample valve was encountered. From the sample valve, the carrier gas flowed through the diffusion column and then through the sensing side of the T.C. cell. The response from the T.C. cell was detected by a Wheatstone bridge circuit.

The continuously recorded response from the T.C. detector cell is said to be linear if the peak area is directly proportional to the concentration of the perturbing component at the detector, or the width at half peak height is constant with respect to the sample size. At low pressures, for all the systems investigated here, the width at half peak height of the short tube was constant with respect to the sample sizes. At high pressures, except for the methane-helium system, the width at half peak height varied a little with the sample sizes. However, the differences in variance between the long and short tubes were nearly the same for different sample sizes.

The exact nature of the response of the T.C. detector is not known. Nogare (*34*) presented an approximate analysis and concluded that the response is governed by the geometry of the detector, the electric circuit, and the thermal conductivities of the gases. Small thermistors and small detector volume give a fast response. The temperature difference between the thermistors and cell wall should be kept small for a linear response. Doebelin (*14*) gave a detailed analysis of the Wheatstone bridge circuits. Under the assumption that the recorder resistance is high, the bridge response is very nearly linear as long as the change of resistance of the sensing leg is a small percentage of the leg resistance. Others (*33, 36*) found an anomalous response over the entire flow rate range studied in their investigations on the behavior of carrier gases of low thermal conductivity.

Ionization Detector. The ionization chamber was constructed at Rice University of Type 303 S.S. for the body and electrodes. The electrode disk surfaces were polished to provide a uniform electric field. The spacer between the electrodes, which contained the bores for the gas flow, was made of Kel-F, a material of high volume resistivity and suitable compressive strength. The sensing volume was about 0.018 cc, with an electrode spacing of 0.8 mm. Teflon was used for seals between the ionization chamber and the outer body of the detector.

Leads from the electrodes were connected to a Cary-31 vibrating reed electrometer, which measured the 10^{-12}-ampere current for continuous recording. Applied voltage across the electrodes came from a regulated d.c. Kepco unit or a Burgess dry cell battery below 5 volts. Linear response was detected and defined (*31*) as the constancy of the variance with respect to the applied voltage.

Recorder. A continuous strip recorder was used to record the signal from the detector cell in use. After preliminary variation, a constant chart speed of 360 inches per hour was adopted. An electric timer, which showed no variation to 0.1 second over a 3-hour period, was used to measure residence times. The human error was estimated to be ± 0.2 second.

The variance was taken as the measured width at half peak height for the thermal conductivity detector. The response from the ionization detector required curve fitting for the width and height, since the recorder output peaks were not quite Gaussian. Measurements on the chart were made with a Vernier caliper manufactured by Brown-Sharpe Co., Switzerland. The instrument's reproducibility was about 0.001 inch, but the estimated human error was 0.003 inch.

EXPERIMENTAL METHOD AND PROBLEMS

The system was repeatedly evacuated and purged with carrier gas. The system lines were charged with carrier gas to the desired pressure and the sample lines were charged with perturbing gas; and the pressures were equalized using valve *PGE* of Figure 2. The bath was raised and the desired operating temperature was established.

Detectors. The thermistors of the T.C. cell required about 4 hours of steady flow to reach a stable condition.

The ionization cell required about 24 hours to achieve steady-state conditions, probably because of an observed (*30, 31, 41*) phenomenon typical of ionization saturation stress current of the insulation materials of the detector. The insulators were treated with an ultrasonic cleaner to help minimize the time to reach steady state. At 50° C the response of the ionization detector showed a large amount of tailing, which invalidated the results. Likewise, at 0° C scattered results were obtained.

The gas flow in the ionization detector passed from ⅛-inch o.d. tubing with 1.8-mm bore through an 0.8-mm hole in the Kel-F spacer into the ionization chamber, then through an 0.8-mm hole back into the ⅛-inch system tubing. The free cross-sectional area for flow varied from 0.025 to 0.005 cm^2 in a length of 12.7 mm. The transition from system tubing to the hole in the Kel-F spacer was a 60° taper, to assist in minimization of the effect of area changes.

Flow. The tandem proportioning pump, by which the mercury entered one cell and left the other at precisely the same rate, provided the desired constant flow rate. Sample injections were made at approximately ¾ of the total residence time computed from Equation 8. Steady-state conditions were assumed when the residence time of the successive injections became constant.

Gases Used. All gases used had high purity. The gas source and purity are given in Table I.

ERROR ANALYSIS

Experimental measurement of any quantity involves possible errors from the particular apparatus and the particular property.

Basic Measurement. The strip chart record from the recorder had to be measured for width w of the peak at height y for Equation 7. The square of the width at half height is proportional to the tube length, and the long tube was approximately four times the length of the short tube. The $\Delta\sigma^2$ in Equation 6 is obtained from the subtraction of two numbers with the same order of magnitude. To minimize this source of error, the experiment was run at least three times for the long tube and six times for the short tube.

Diffusivity is a function of concentration and therefore is dependent on the measurement of the average value over the concentration range of the experiment. This source of error was decreased by using a sufficiently long "short tube" so that the perturbing gas concentration was less than 1% by volume in the elution gas.

Table I. Experimental Gases

Gas	Mole %	Gas Source	Reference for Density
Elution			
Helium	99.995	Bureau of Mines Helium Plant, Amarillo, Tex.	(*8, 42*)
CF_4	99.86	Du Pont Co.	(*15*)
CH_4	99.9+	Matheson Co.	(*16*)
Perturbation			
CH_4	99.9+	Matheson Co.	
CH_3T	...	New England Nuclear Corp.	
CO_2	99.9+	Matheson Co.	
Ar	99.9+	Matheson Co.	
N_2	99.9+	Matheson Co.	

Figure 3. Additivity of variance for ionization detector for $CH_3T^{\infty} \rightarrow CH_4$ at 25° C, 28 atm, 80 cc per hour

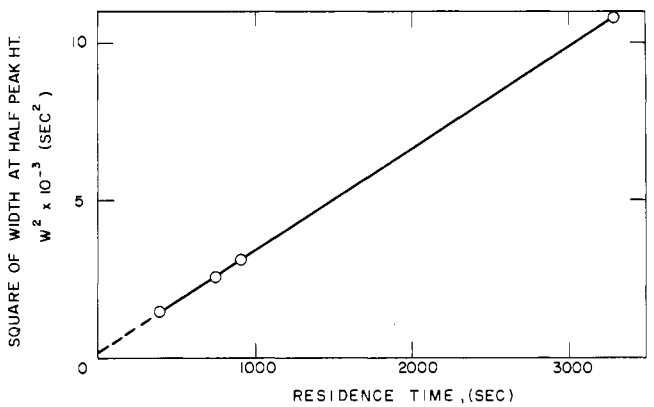

Figure 4. Additivity of variance for thermal conductivity detector for $Ar^{\infty} \rightarrow$ He at 50° C, 50 atm, 40 cc per hour

Figures 3 and 4 indicate that linearity was obtained for each detector and these errors were minimized.

Geometry of Diffusion System. Flow in a coil induces additional effects which are not present in a straight tube. Koutsky and Adler (27) concluded that the dispersion in helical tubes approximates that in straight tubes for Reynolds number less than 300. Others (1) have shown that the effect of a coiled column becomes evident for gaseous dispersion systems only for Reynolds number greater than 100. No clear evidence has been found to relate the ratio of tube-to-column diameters to the flow in the tube. The ratio of the diameters for this apparatus was 0.02, and operating conditions were well below a Reynolds number of 100. Typical results shown in Figure 5 indicate that no coiling effect was present in these studies.

Another geometrical effect arises from the initial disturbance of the perturbation. This was reduced or perhaps eliminated by subtraction of the measurements on the long tube and the short tube.

The geometry of the detector could also be a source of error. The sensitivity of the thermistors in the T.C. cell limited the Reynolds number to about 5. Taylor's diffusion did not contribute more than a maximum of 10% to the effective diffusion. Figures 3 and 4, along with the independence of diffusivity with flow rate shown in Tables IV and V of the results, indicate that error due to geometry of the detector was negligible.

RESULTS

Complete information on this investigation is available (25). Typical fundamental experimental measurements are

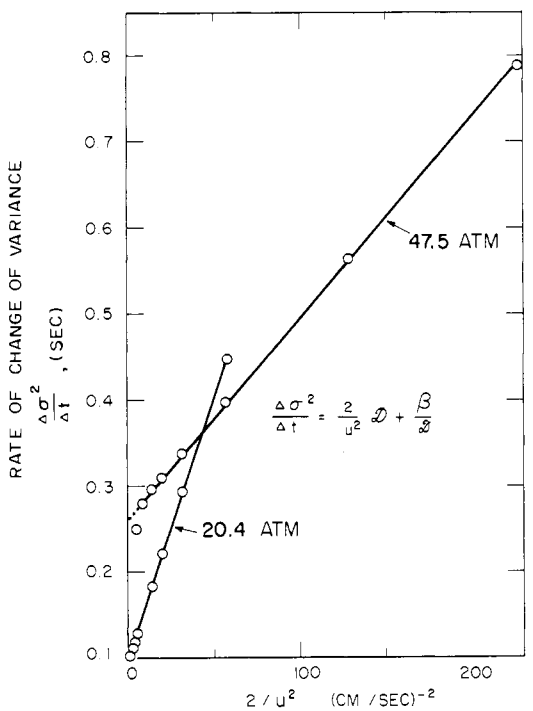

Figure 5. Determination of diffusivity of $CH_3T^{\infty} \rightarrow CF_4$ at 25° C

Table II. Diffusivity Results for Infinitesimal Pulse of CH_3T in CH_4 at 25° C, Multiflow Rate Method

P, Atm	$\mathcal{D}$, Cm^2/Sec	CH_4 Density, ρ, (G/Cc) $\times 10^4$	$\rho\mathcal{D}$, (G/Cm-Sec) $\times 10^4$	N
2.04	0.106	13.4	1.42	4
6.78	0.0319	45.2	1.44	4
20.4	0.0100	139	1.39	4
33.9	0.00598	236	1.42	4
47.5	0.00429	338	1.45	3
61.1	0.00323	445	1.44	2

Table III. Diffusivity Results for Infinitesimal Pulse of CH_3T in CF_4 at 25° C, Multiflow Rate Method

P, Atm	$\mathscr{D}$, Cm^2/Sec	CF_4 Density, ρ, (G/Cc) $\times 10^4$	$\rho\mathscr{D}$, (G/Cm-Sec) $\times 10^4$	$\beta \times 10^3$, Cm^2	N
2.05	0.0688	74.8	5.15	[a]	3
6.78	0.0204	250	5.10	[a]	5
20.4	0.00643	794	5.10	0.593	8
33.9	0.00373	1386	5.17	0.601	8
47.5	0.00240	2072	4.97	0.598	8
61.1	0.00177	2823	5.00	0.592	6

Theoretical β from Equation 9 = 0.591

Typical Basic Experimental Data for 61.1 Atm

Flow Rate, Cc/Hr	Residence Time, Sec		Width at Half Peak Height[b], Sec	
	Long tube	Short tube	Long tube	Short tube
12.5	10480.0	4261.0	235.9	156.1
15	8729.0	3550.5	193.9	128.1
20	6551.0	2663.4	146.8	96.39
30	4367.1	1776.2	105.5	68.35
40	3274.7	1332.7	86.38	55.87
80	1637.6	667.0	56.07	35.64

[a] Veracity of β questionable, since data are at high flow rates. [b] Correlated value using Equation 7.

Table IV. Diffusivity Results for Infinitesimal Pulse of Ar in He, One-Flow Rate Method with Constant Pressure Check Runs of Multiflow Rate Method

t, ° C	P, Atm	$\mathscr{D}$, Cm^2/Sec	He Density, ρ, (G/Cc) $\times 10^3$	$\rho\mathscr{D}$, (G/Cm-Sec) $\times 10^4$
50	59.8	0.0145	8.808	1.28
	49.8	0.0175	7.365	1.29
	29.9	0.0288	4.458	1.28
	9.97	0.0851	1.498	1.27
25	59.8	0.0127	9.523	1.21
	49.8	0.0152	7.966	1.21
	29.9	0.0249	4.826	1.20
	9.97	0.0742	1.623	1.20
0	59.8	0.0109	10.34	1.13
	49.8	0.0130	8.661	1.13
	29.9	0.0215	5.225	1.13
	9.97	0.0634	1.771	1.12
−25	59.8	0.00931	11.34	1.06
	49.8	0.0111	9.506	1.05
	29.9	0.0184	5.774	1.06
	9.97	0.0541	1.948	1.05

Check Runs with Multiflow Rate Method at 10 Atm

	Flow Rate, Cc/Hr			
50	50	0.0847		
	80	0.0845		
	100	0.0845		
	120	0.0847		
	Av.	0.0846	1.503	1.27
25	40	0.0737		
	50	0.0739		
	60	0.0738		
	80	0.0737		
	100	0.0739		
	120	0.0736		
	160	0.0738		
	Av.	0.0738	1.629	1.20
0	50	0.0636		
	80	0.0637		
	100	0.0635		
	120	0.0636		
	Av.	0.0636	1.778	1.13
−25	50	0.0543		
	80	0.0545		
	100	0.0542		
	120	0.0544		
	Av.	0.0543	1.954	1.06

Table V. Diffusivity Results for Infinitesimal Pulse of CH_4 in He, One-Flow Rate Method, with Constant Temperature Check Runs of Multiflow Rate Method

t, ° C	P, Atm	$\mathscr{D}$, Cm^2/Sec	He Density, ρ, (G/Cc) $\times 10^3$	$\rho\mathscr{D}$, (G/Cm-Sec) $\times 10^4$
50	59.8	0.0134	8.808	1.18
	49.8	0.0159	7.365	1.17
	29.9	0.0265	4.458	1.18
	9.97	0.0781	1.498	1.17
25	59.8	0.0117	9.523	1.11
	49.8	0.0139	7.966	1.11
	29.9	0.0229	4.826	1.10
	9.97	0.0681	1.623	1.10
0	59.8	0.0101	10.34	1.04
	49.8	0.0119	8.661	1.03
	29.9	0.0198	5.255	1.04
	9.97	0.0588	1.771	1.04
−25	59.8	0.00872	11.34	0.990
	49.8	0.0103	9.506	0.978
	29.9	0.0169	5.774	0.977
	9.97	0.0501	1.948	0.976

Check Runs with Multiflow Rate Method at 25° C

P, Atm	Flow Rate, Cc/Hr			
6.8	140	0.100		
	160	0.100		
	200	0.100		
	240	0.101		
	Av.	0.100	1.108	1.11
20.4	100	0.0335		
	120	0.0335		
	140	0.0333		
	160	0.0338		
	Av.	0.0335	3.305	1.11
33.9	60	0.0204		
	80	0.0203		
	100	0.0205		
	120	0.0207		
	Av.	0.0205	5.453	1.12
47.5	40	0.0147		
	50	0.0144		
	60	0.0147		
	80	0.0147		
	Av.	0.0146	7.595	1.11
61.1	35	0.0115		
	40	0.0114		
	50	0.0114		
	60	0.0115		
	Av.	0.0114	9.710	1.11

given in the second part of Table III. The numerical results are presented in Tables II through VI. Graphical representations for 1 atm with results of other investigators are shown in Figures 6 and 7. The eluting gas density calculation used the second virial coefficient for helium and the Benedict-Webb-Rubin equation for methane and tetrafluoromethane, with the constants evaluated from the data sources given in Table I.

Multiflow Rate Method. The radioactive perturbations with tritiated methane in methane and tetrafluoromethane at 25° C were evaluated by Equation 9 for the multiflow rate method (Tables II and III). Each datum represents two to eight experimental measurements.

In addition, the multiflow rate method was used as a check at constant pressure for the argon and at constant temperature for the methane perturbations in helium (Tables IV and V). The results from the two methods agree.

One-Flow Rate Method. The diffusion of argon, methane, nitrogen, and carbon dioxide, respectively, in helium at 50°, 25°, 0°, and −25° C up to 60 atm was measured using

Table VI. Diffusivity Results for Infinitesimal Pulse of N_2 in He and of CO_2 in He, One-Flow Rate Method

t, °C	P, Atm	$\mathscr{D}$, Cm^2/Sec	He Density, ρ, (G/Cc) $\times 10^3$	$\rho\mathscr{D}$, (G/Cm-Sec) $\times 10^4$
		NITROGEN		
50	59.8	0.0140	8.808	1.23
	49.8	0.0166	7.365	1.22
	29.9	0.0272	4.458	1.21
	9.97	0.0820	1.498	1.23
0	59.8	0.0105	10.34	1.09
	49.8	0.0124	8.661	1.08
	29.9	0.0206	5.255	1.08
	9.97	0.0607	1.771	1.07
−25	59.8	0.00889	11.34	1.01
	49.8	0.0107	9.506	1.02
	29.9	0.0177	5.774	1.02
	9.97	0.0522	1.948	1.02
		CARBON DIOXIDE		
50	49.8	0.0141	7.365	1.04
	39.8	0.0177	5.910	1.05
	29.9	0.0236	4.458	1.05
	9.97	0.0701	1.498	1.05
25	49.8	0.0127	7.966	1.01
	39.8	0.0156	6.395	1.00
	29.9	0.0206	4.826	1.00
	9.97	0.0616	1.623	1.00
0	49.8	0.0107	8.661	0.928
	39.8	0.0133	6.958	0.925
	29.9	0.0177	5.255	0.931
	9.97	0.0525	1.771	0.929
−25	49.8	0.00920	9.506	0.874
	39.8	0.0116	7.641	0.883
	29.9	0.0151	5.774	0.873
	9.97	0.0454	1.948	0.885

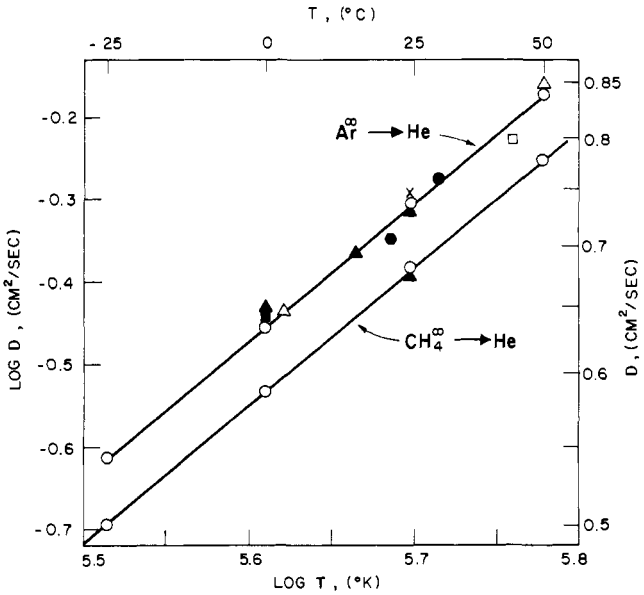

Figure 6. Comparison of results of various investigators for $Ar^{\infty} \rightarrow He$ and $CH_4^{\infty} \rightarrow He$ at 1 atm

- O This work
- ■ (12)
- ▲ (37)
- △ (32)
- ● (21, 22)
- ● (39)
- □ (24)
- X (40)

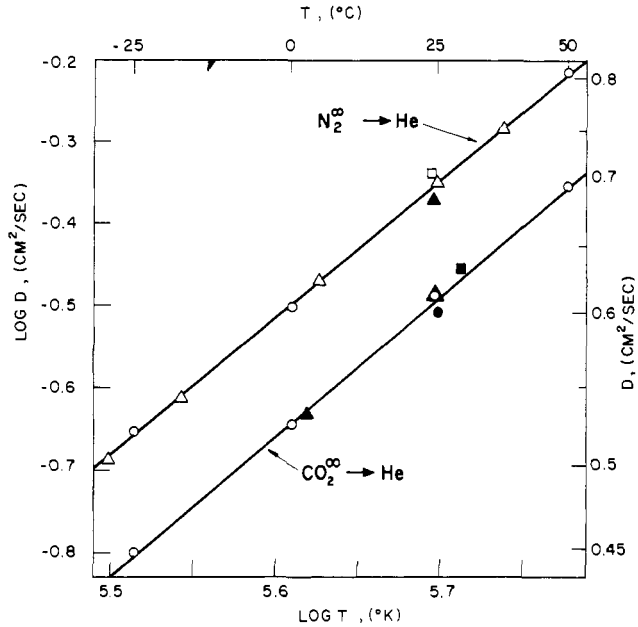

Figure 7. Comparison of results of various investigators for $N_2^{\infty} \rightarrow He$ and $CO_2^{\infty} \rightarrow He$ at 1 atm

This work
- O (11)
- △ (37)
- ▲ (38)
- □ (39)
- ■ (24)

Table VII. Comparison with Results of Other Investigations

System	Diffusivity at 25° C and 1 Atm, Cm^2/Sec	Reference
$CH_4^{\infty} \rightarrow CH_4$	0.207	(45)[a]
	0.227 ± 0.006	(13)[a]
	0.228 ± 0.005	(46)[a]
	0.224 ± 0.004	This work[a,b]
$CH_4^{\infty} \rightarrow CF_4$	0.139	(37)[c]
	0.141 ± 0.003	This work[a,b]
$AR^{\infty} \rightarrow He$	0.729	(40)
	0.753	(32)[d]
	0.734 ± 0.007	This work[a]
$CO_2^{\infty} \rightarrow He$	0.612	(40)
	0.621	(26)[d]
	0.612 ± 0.006	This work[a]
$CH_4^{\infty} \rightarrow He$	0.675	(9)
	0.679 ± 0.006	This work[a]

[a] Values calculated from smoothed values of density-diffusivity product. [b] Values calculated from tritiated methane data with mass correction factor (23). [c] Calculated from Chapman-Enskog theory. [d] Interpolated.

Equation 10, except that nitrogen in helium was not investigated at 25° C. (Tables IV through VI).

The values for the diffusivity at 1 atm for the four systems calculated from the density-diffusivity products are shown in Figures 6 and 7 for comparison with other investigators.

Analysis of Results. Experimental data can be examined internally by error analysis to evaluate the precision of the particular system. The results of the error analysis at 25° C are given in Table VII, which also gives results of other investigators for comparison. There are several sources of inherent experimental error common to all diffusivity measurements. The estimation of the error shown

in Table VII varies from 1 to 3%, which is sufficient to account for the variation in results at infinite dilution from different investigations shown in Figures 6 and 7.

Another test of the validity of experimental results is a comparison with theoretical prediction, given in Table III for the tritiated methane in tetrafluoromethane system, where the experimental value of β at the four highest pressures is given. The theoretical prediction of β from Equation 9 agrees satisfactorily with the experimental results.

ACKNOWLEDGMENT

Bath fluids were donated by the Union Carbide Chemical Corp. and Phillips Petroleum Co., and the tetrafluoromethane was donated by E. I. du Pont de Nemours & Co. Patsy S. Chappelear made many valuable suggestions and helped in the preparation of the manuscript.

NOMENCLATURE

C = concentration of tracer gas in carrier gas
$\bar{C}$ = mean concentration over cross section of tube
$\mathscr{D}$ = molecular diffusion coefficient, cm^2/sec
$\mathscr{D}_e$ = effective diffusion coefficient, cm^2/sec
L = tube length between injection point and measurement point, cm
N = number of experimental data
O = order of magnitude
P = absolute pressure
Pe = Peclet number, $2\bar{u}r_t/\mathscr{D}$
T = absolute temperature, °K
T.C. = thermal conductivity
a_1, a_2, a_3 = constants with respect to tube length
m_2 = second moment, $\int_0^1\int_{-\infty}^{+\infty}x_1^2C\,dx_1\rho d\rho/\int_0^1\rho d\rho$
r = radial coordinate, cm
r_t = radius of tube, cm
t = time, sec
t_R = residence time, sec
$\bar{t}$ = mean time, $\int_0^\infty t\int_0^1C\rho d\rho dt/\int_0^\infty\int_0^1C\rho d\rho dt$, sec
$\bar{u}$ = average velocity, $2\int_0^1u\rho d\rho$, cm/sec
w = peak width at height y
x_1 = dimensionless axial coordinate moving with center of mass of tracer, $(z-\bar{u}t)/r_t$
y = height at peak width w
z = axial coordinate measured from injection point, cm

Greek Letters

α = parameter, $\mathscr{D}_e/(\bar{u}\,L)$
σ^2 = variance, defined as $\int_0^\infty(t-\bar{t})^2\int_0^1C\rho d\rho dt/\int_0^\infty\int_0^1C\rho d\rho dt$, time^2
ρ = dimensionless radial coordinate, r/r_t, in equations
$\rho\mathscr{D}$ = density-diffusivity product, g/cm-sec
τ = dimensionless time variable, $t\mathscr{D}/r_t^2$
Δ = difference, long tube − short tube
β = constant defined in Equation 9, determined by set of flow rate measurements, cm^2

Subscripts

o = at injection position or point
L = at measurement or detection point
t = at inside radius of tube

Superscript

∞ = infinite dilution—i. e., very small sample injection

LITERATURE CITED

(1) Andel, E. van, Kramers, H., Voogd, A. de, *Chem. Eng. Sci.* **19**, 77 (1964).
(2) Arai, K., Saito, S., Maeda, S., *Chem. Eng. (Japan)* **32**, 54 (1968).
(3) Aris, R., *Proc. Roy. Soc. (London)* **A235**, 67 (1956).
(4) *Ibid.*, **A245**, 268 (1958).
(5) Bischoff, K.B., *Chem. Eng. Sci.* **12**, 69 (1960).
(6) Bischoff, K.B., Levenspiel, O., *Ibid.*, **17**, 257 (1962).
(7) Bournia, A., Coull, J., Houghton, G., *Proc. Roy. Soc. (London)* **A261**, 227 (1961).
(8) Canfield, F., Leland, T.W., Kobayashi, R., J. CHEM. ENG. DATA **10**, 92 (1965).
(9) Carswell, A.J., Stryland, J.C., *Can. J. Phys.* **41**, 708 (1963).
(10) Chang, G.T., Ph.D. thesis, Rice University, Houston, Tex., 1966 (available from University Microfilms).
(11) Chang, G.T., Kobayashi, R., XXXVI International Congress on Industrial Chemistry, Brussels, Sept. 10-21 (1966); *G.II-S.4-571 Maison d'Edition S. C., Marcinelle.*
(12) Chapman, S., Cowling, T.G., "The Mathematical Theory of Non-uniform Gases," Cambridge University Press, London, New York, 1951.
(13) Dawson, R., Ph.D. thesis, Rice University, Houston, Tex., 1966.
(14) Doebelin, E.O., "Measurement Systems: Application and Design," McGraw-Hill, New York, 1966.
(15) Douslin, D.R., *J. Chem. Phys.* **35**, 1357 (1961).
(16) Douslin, D.R., Harrison, R.H., Moore, R.T., McCullough, J.P., J. CHEM. ENG. DATA **9**, 358 (1964).
(17) Evans, E.V., Kenney, C.N., *Proc. Roy. Soc. (London)* **A284**, 540 (1965).
(18) Giddings, J.C., Seager, S.L., *Ind. Eng. Chem. Fundamentals* **1**, 277 (1962).
(19) Gill, W.N., Ananthakrishnan, K., *A.I.Ch.E. J.* **13**, 801 (1967).
(20) Golay, M.J.E., "Gas Chromatography," p. 36, Butterworths, London, 1958.
(21) Heijningen, R.J. van, Ph.D. thesis, University of Leiden, Netherlands, 1967.
(22) Heijningen, R.J.J. van, Harpe, J.P., Beenakker, J.J.M., *Physica* **38**, 1 (1968).
(23) Hirschfelder, J.O., Curtiss, C.F., Bird, R.B., "Molecular Theory of Gases and Liquids," 2nd ed., Wiley, New York, 1964.
(24) Holsen, J.N., Strunk, M.R., *Ind. Eng. Chem. Fundamentals* **3**, 143 (1964).
(25) Hu, A.T., Ph.D. thesis, Rice University, Houston, Tex., 1969 (available from University Microfilms, Ann Arbor, Mich.).
(26) Ivakin, B.A., Suetin, P.E., *Zh. Tekhn. Fiz. (Soviet Phys., Tech. Phys.)* **34**, 1115 (1964).
(27) Koutsky, J.A., Adler, R.J., *Can. J. Chem. Eng.* **42**, 239 (1964).
(28) Laan, E. Th. van der, *Chem. Eng. Sci.* **7**, 187 (1958).
(29) Levenspiel, O., Smith, W.K., *Ibid.*, **6**, 227 (1957).
(30) Loeb. L.B., "Basic Processes of Gaseous Electronics," University of California Press, Los Angeles, 1960.
(31) Lovelock, J.E., *Anal. Chem.* **33**, 162 (1961).
(32) Malinauskas, A.P., *J. Chem. Phys.* **42**, 157 (1965).
(33) Miller, J.M., Lawson, A.E., Jr., *Anal. Chem.* **37**, 1348 (1965).
(34) Nogare, S.D., Juvet, R.S., Jr., "Gas-Liquid Chromatography," Interscience, New York, 1962.
(35) Opfell, J.B., Sage, B.H., *Ind. Eng. Chem.* **47**, 918 (1955).
(36) Pecsok, R.L., Windson, M.L., *Anal. Chem.* **40**, 92 (1968).
(37) Reid, R.C., Sherwood, T.K., "The Properties of Gases and Liquids," McGraw-Hill, New York, 1966.
(38) Rumpel, W.F., University of Wisconsin Naval Research Laboratory, Rept. **CM-851** (1955).
(39) Saxena, S.C., Mason, E.A., *Mol. Phys.* **2**, 379 (1959).
(40) Seager, S.L., Geertson, L.R., Giddings, J.C., J. CHEM. ENG. DATA **8**, 168 (1963).
(41) Sharpe, J., "Nuclear Radiation Detectors," Methuens, London, 1964.
(42) Stroud, L., Miller, J., Brandt, L.W., J. CHEM. ENG. DATA **5**, 51 (1961).
(43) Taylor, G., *Proc. Roy. Soc. (London)* **A219**, 186 (1953).
(44) *Ibid.*, **A225**, 473 (1954).
(45) Timmerhaus, K.D., Drickamer, H.G., *J. Chem. Phys.* **19**, 1242 (1951).
(46) Trappeniers, N.J., Oosting, P.H., *Phys. Letters* **23**, 445 (1966).

RECEIVED for review September 29, 1969. Accepted February 9, 1970. 66th National Meeting, A.I.Ch.E., August 24 to 29, 1969, Portland, Ore. Work supported by the National Science Foundation.